Indian J. Met. Hydrol. Geophys. (1978), **29**, 1 & 2, 187-197

551·553·21 : 551·513 : 551·576·3 (215-17)

*Fluctuations in the northern hemispheric winter circulations**

TAKIO MURAKAMI and MANAKKAMPAD S. UNNINAYAR

Department of Meteorology, University of Hawaii, Honolulu, Hawaii

ABSTRACT. Between 12 and 16 January 1971, exceptionally large cloudiness was observed over Malaysia and Indonesia. The 700 mb winds over the western North Pacific and south China Sea between about 15°N and the equator, normally easterlies, were replaced by somewhat strong westerlies. Concurrently, near Japan (South Australia) the jet stream at 700 mb diminished (increased) substantially in speed. Below normal cloudiness was observed over eastern Asia, perhaps reflecting weak surface monsoonal surges over that region. At 200 mb, the E-W divergent circulations became well established over the equatorial western Pacific, presumably carrying excess energy supplied over the Indonesian region very far downstream to the equatorial central Pacific dry zone.

From 19 to 23 January 1971, below normal cloudiness existed over Malaysia and Indonesia in contrast to well above normal cloudiness over the south Indian Ocean and South Africa between about 5°S and 15°S. During that period, near equatorial westerlies at 700 mb disappeared from the Malaysian region, while they intensified over the equatorial Indian Ocean. At 200 mb, the jet stream near and to the east of Japan was exceptionally weak. Over the equatorial central Pacific, the E-W divergent circulation became ill defined, while N-S overturnings were more active than usual.

1. Introduction

Considerable weather fluctuations occur over the Malaysian region during the northern winter despite the rarity of vigorous tropical storms and moving disturbances. The majority of occasions of heavy precipitation over the Malaysian region are due to weak depressions developing along the low-level near-equatorial trough (Bryant 1958). These depressions are possible when the northeast trades are sufficiently broad and deep, surging southsouthwestwards from the north of the south China Sea and ultimately merging with the near-equatorial trough and equatorial westerlies. Concurrently, the upper tropospheric subtropical ridge system is well organized and displaced slightly northwards of its normal position (Ramage 1968).

Dry weather over the Malaysian region appears to be associated with two distinct circulation phases. During some dry spells, the upper subtropical ridge is displaced southwards of its normal position and becomes ill defined when upper troughs in the westerlies penetrate southwards to equatorial latitudes. The weather associated with the equatorial part of the upper trough is clear owing to the presence of dry air in and around the trough (Liang 1974). Over Indochina and the northern part of the south China Sea precipitation is found to the east of the subtropical part of extended troughs.

Other dry spells are of a different character and are associated with a very rapid deepening upper troughs well into the southern hemisphere. The surface northeasterly trades are strong and converge into developing disturbances in the southern hemisphere near-equatorial trough (Bryant 1958). In such instances, convective activity seems to be most pronounced to the south of the Java-New Guinea area. Limited research on the Australian summer monsoon has revealed that when rains are weaker over the Malaysian and Indonesian region, low-level flow across the equator into Australia is apparently stronger than normal, tending to increase the rainfall over northern Australia.

*Contribution No. 76-13 of the Department of Meteorology, University of Hawaii.

Most of the synotpic studies cited above have concentrated on circulation changes over local areas such as the east and south China Seas, Malaysia and Indonesia, and a part of the southern hemisphere near Australia. It is quite probable, however, that the weather fluctuations over the Malaysian and Indonesian regions are intimately related to much larger scale global circulation changes. This possibility, central to the present study, is examined by using wind data at 200 mb and 700 mb compiled by the National Meteorological Centre, NOAA, together with satellite derived cloudiness data as unique parameters providing continuous space and time coverage over the atmosphere.

2. Data and computational procedures

List of symbols

λ	longitude
θ	latitude
a	radius of earth
u, v	zonal and meridional winds
c	cloudiness amount
ϕ	geopotential
ψ	streamfunction
χ	velocity potential
$(\bar{\ })$	zonal mean
$(\ )'$	departure from zonal mean
$< >$	time mean
$(\ )^*$	departure from time mean
k^*	transient eddy kinetic energy

To investigate the changes in atmospheric circulations during the northern winter, u and v data at 200 mb and 700 mb from December 1970 through February 1971, determined by operational analysis at the National Meteorological Centre (NMC), were used. During this 90-day period, both commercial aircraft and ATSI/ATS3 data were utilized in the NMC operational analysis. We, therefore, felt that the NMC data may be realistic enough to resolve at least the large-scale aspects of circulation changes during the northern winter. Wind analyses are available for the NMC 73×23 point tropical grid, equally spaced on a mercator projection, from 48·09°S to 48·09°N. The fields of divergence as derived from the NMC wind analysis are probably somewhat smoothed, being intended for use as initial data to the NMC weather prediction models. Thus, the divergence fields associated with smaller scale disturbances may not be too realistic. However, note that daily maps of the upper circulation during the northern winter are known to contain primarily long wave features.

The daily NMC wind data was used comparatively with cloudiness data as determined by Prof. Sadler (University of Hawaii) over 2·5 degree latitude-longitude grid squares between 30°S and 30°N [The manner of data extraction is described in Sadler (1968) and Atkinson and Sadler (1970)]. Horizontal smoothing was applied to the original data over a 5° Lat./5° Long. area to eliminate small-scale noise while retaining large-scale cloudiness perturbations of specific interest. As shown later, changes in observed divergence (or velocity potential) agreed reasonably well with those in cloudiness during the northern winter.

Daily u, v and c data were separated into zonal mean and eddy components. For example, u was expressed as

$$u = \bar{u} + u' \tag{1}$$

Introducing the notation $< >$ to represent the time mean value for the northern winter and $(\ )^*$ the departure from it :

$$u = < \bar{u} > + u^* \tag{2}$$

Thus, u^* is defined as the transient component of u.

The same procedure for the separation of horizontal winds into rotational and divergent wind components as described by Krishnamurti *et al.* (1973) was employed in the present study; *i.e.*, streamfunction ψ was obtained by

$$\nabla^2 \psi' = \frac{\partial v'}{a \cos\theta \, \partial\lambda} - \frac{\partial u' \cos\theta}{a \cos\theta \, \partial\theta} \tag{3}$$

$$\bar{\psi} = -\int \bar{u} \, a \, d\theta \tag{4}$$

In solving the Poisson equation (3) we have assumed that $\psi' = \phi'/f$ at 48.1°N and 37.1°S. The daily ϕ'-values at the boundaries were determined numerically from temperature data prepared by U.S. Navy Fleet Numerical Weather Center. When integrating equation (4), $\bar{\psi}$ was assigned to be zero at the equator.

Likewise, the velocity potential χ was obtained by

$$\nabla^2 \chi' = \frac{\partial u'}{a \cos\theta \, \partial\lambda} + \frac{\partial v' \cos\theta}{a \cos\theta \, \partial\theta} \tag{5}$$

$$\bar{\chi} = \int \bar{v} \, a \, d\theta \tag{6}$$

where $\chi' = 0$ was prescribed at 48.1°N and 37.1°S, and $\bar{\chi} = 0$ at the equator.

The transient eddy kinetic energy was computed at every NMC grid point (approximately 5 degree latitude-longitude) as follows :

$$k^* = \frac{1}{2} \langle u^{*2} + v^{*2} \rangle \qquad (7)$$

3. Winter mean circulations

The 90-day mean streamfunction and velocity potential were computed from Eqns. (3) to (6) at both 200 mb and 700 mb. These fields were then used to compute the non-divergent and divergent parts of the mean winds during the northern winter. Fig. 1 shows the distribution of the mean non-divergent winds at 200 mb. One notes the existence of a strong jet stream near Japan with a maximum (72 m sec^{-1}) around 33°N, 135°E. To the north (south) of this jet stream is a pronounced trough (ridge) system. The subtropical ridge centres near 15°N, 135°E. Similar features are also noted along the east coast of North America with a trough in higher latitudes, a ridge system in tropical latitudes and a somewhat strong (48 m sec^{-1} at 37°N, 75°W) jet stream in intervening latitudes.

The existence of strong westerlies over the equatorial central Pacific (23 m sec^{-1} at 135°W) is particularly conspicuous. Equatorial westerlies, while considerably weaker, are also present over the Atlantic Ocean. The upper tropospheric westerlies over the equatorial Pacific are directly related to oceanic troughs existing in both the North and South Pacific. The winds associated with these troughs become predominantly zonal as the equator is approached. The strong westerlies near 135°W at the equator are associated with the confluence of nondivergent northerly (southerly) flows to the west of the northern (southern) hemisphere trough; namely, the increase (decrease) of non-divergent westerly winds along the equator to the west (east) of 135°W is not associated with horizontal divergence, but is due to the confluence (difluence) of the non-divergent winds in and around mid-oceanic troughs over the North and South Pacific.

Fig. 2 depicts the divergent part of the mean winds at 200 mb. The divergent winds are southwesterly over the equatorial western Pacific while they are easterly or southeasterly over the equatorial eastern Pacific. The divergent southwesterlies attain maximum speeds (2·7 m sec^{-1}) around 165°E at the equator. East of that longitude, strong downdraft beneath convergent flows favours

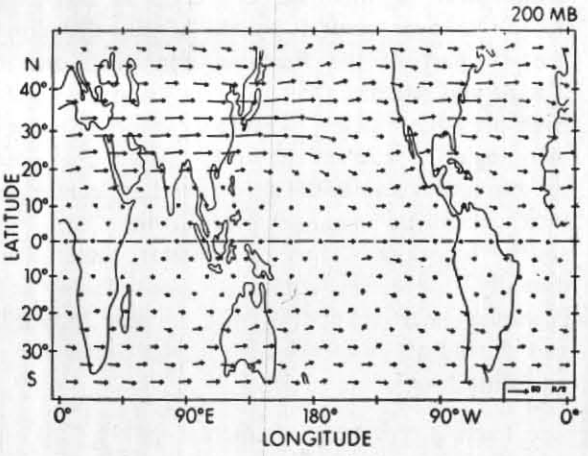

Fig. 1. 200 mb winter mean non-divergent wind vector field during the period from December 1970 to February 1971. Arrows originate from individual grid points. (This applies to all figures showing vector fields).

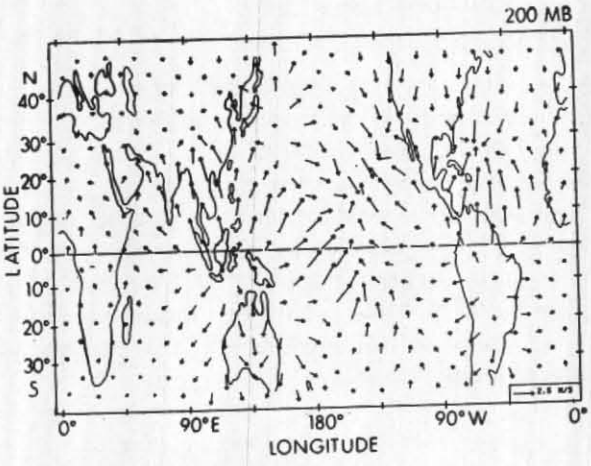

Fig. 2. 200 mb winter mean divergent wind vector field

persistent cloudless sky and dry weather. This equatorial divergent circulation may correspond to the so-called Walker circulation, characterized by predominantly wet climate to its west (Malaysia and Indonesia) and dry weather to its east (central Pacific).

In Fig. 2, two distinct regions of large divergence are found in equatorial latitudes, centred over the Indonesian region near 5°S, 120°E and the northwestern part of South America near 10°S, 70°W. Although it is not clear in Fig. 2, upper divergence is also substantial over central South Africa near 10°S, 35°E. These are three of the most active convective regions in the tropics during the northern winter. The divergent winds at 200 mb emanate

from these regions and converge around 20°N to 30°N, over central North Africa, the northeastern part of the Eurasian continent, and the Pacific and Atlantic Oceans directly above surface high pressure systems. Outflow from the Indonesian region is carried off both toward the north as southerlies and south as northerlies, converging into continental regions over north China and south Australia. Thus, a planetary-scale, meridionally oriented circulation (local Hadley cell) is implied with an updraft portion near Indonesia and downdraft branches over north China as well as south Australia.

Yet another feature of interest in Fig. 2 is the existence of a marked band of large divergence extending southeastwards from the east of New Guinea to the central South Pacific near 25°S, 135°W. This band is nearly coincident with a region of large cloudiness during the northern winter. Much of the upper outflow from this large cloudiness region blows off to the northeast and converge into the equatorial central Pacific.

At 700 mb (Fig. 3), a well organised ridge system extends all the way around the globe along about 20°N. To the north of this ridge axis are westerly winds with a speed maximum (18 m sec^{-1}) near the east coast of North America around 37°N, 75°W. Near Japan, however, the westerlies are much weaker, amounting to only about 13 m sec^{-1} at 30°N, 135°E. Over that region the vertical wind shear, as measured by the difference in the nondivergent winds at 200 mb and 700 mb is approximately 60 m sec^{-1}. This value must be compared with the corresponding value of 30 m sec^{-1} near the east coast of North America. Therefore, it is probable that local baroclinic processes are more active over the former than the latter region.

Between about 15°N and the equator, easterlies prevail with cyclonic shear near 5°N where the near equatorial cloudiness zone (or ITCZ) exists. Cyclonic shear is largest ($>10^{-5}$ sec^{-1}) near the south China Sea. Over the equatorial Indian Ocean, Malaysia and the north Borneo region, the near equatorial trough is clearly seen locating between 2°-5°N with equatorial westerlies to its south. The southern hemisphere trough at 700 mb lies east-west along about 10°S from the western Indian Ocean to the north Australian region where the southern summer monsoon is at a maximum intensity. South of this trough is a well organized high cell centring over northwestern

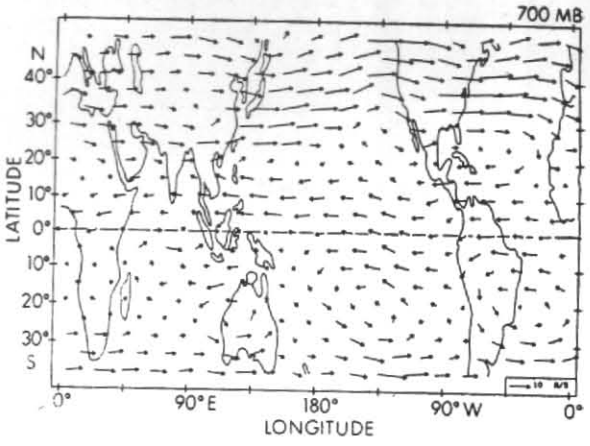

Fig. 3. 700 mb winter mean non-divergent wind vector field

Australia, a part of the southern hemispheric subtropical ridge system extending all the way around the globe along about 20°S.

As expected, the divergent component of the mean winds at 700 mb converge into the Indonesian region (Fig. 4). The centre of convergence is located to the east of Borneo near 2·5°S, 120°E (Conspicuously, most of the inflow comes from the north, west and south. Why only a minor portion is due to inflow from the east is not yet known). It appears that the largest contribution to this convergence is that due to southerly winds originating from the Australian summer monsoon region. Also note the existence of strong divergence over the equatorial south central Pacific where the downdraft leg of the Walker circulation is encountered.

Fig. 5 (top) shows a longitude-latitude section of transient eddy kinetic energy k^* at 200 mb computed from Eq. (7) for January 1971 when the winter monsoon was most intense. k^* is notably small over the tropical latitudes between about 15°S and 10°N. In contrast, large k^* is found over a broad mid-latitude region extending from Japan, through the North Pacific and North America, to the western North Atlantic between 30°N and 45°N. In this region the upper tropospheric jet stream frequently changes its intensity and location as shown later. Another feature of interest is a marked band of relatively large transient eddy kinetic energy over the central North and South Pacific extending across the equator around 160°W. This band nearly coincides with the axis of the mid-oceanic troughs, embedded in westerlies over the North and South Pacific. During the

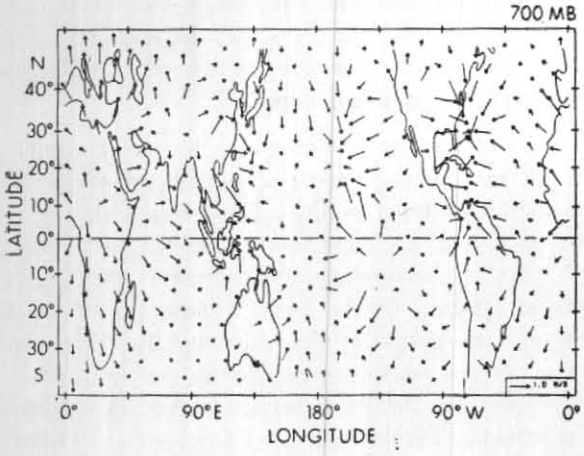

Fig. 4. 700 mb winter mean divergent wind vector field

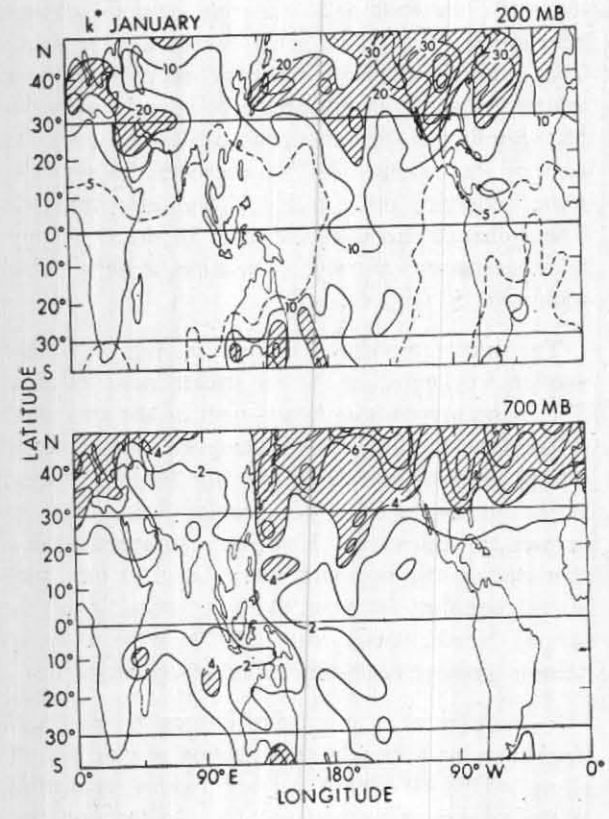

Fig. 5 (Top) : Transient eddy kinetic energy at 200 mb computed from Eq. (7) in units of $10\,m^2\,sec^{-2}$. Interval 10 units. Shading indicates regions where k^* exceeds 20 units.

(Bottom) : k^* at 700 mb. Interval 2 units. Regions of $k^* > 2$ units are shaded.

northern winter, the position and intensity of the oceanic troughs are subject to some variation, sometimes facilitating the development of cyclonic vortices in and around the troughs. Occasionally, mid-atitude systems in the northern hemisphere westerlies penetrate far southwards, resulting in anomalous variations in the intensity of equatorial westerlies over the central Pacific. This point will be elaborated on in the next section.

At 700 mb too, transient eddy kinetic energy is substantially large over the central North Pacific between 30°N and the equator along about 160°W. This is consistent with our synoptic experience of considerable weather fluctuations that occur near the Hawaiian Islands during the northern winter. In Fig. 5 (bottom), a marked band of large transient eddy kinetic energy extends along about 135°E from Japan to the north of Borneo. Undoubtedly, this is associated with monsoonal cold surges bursting out of the Siberian high. When the northeast cold surge is extremely strong, it penetrates deep into the southern hemisphere (Bryant 1958). Whether such cross-equatorial incursions can really result in significant interactions between the two hemispheres is a matter of conjecture and certainly worth further study.

Of interest is the existence of large transient kinetic energy at 700 mb over the central Indian Ocean with a maximum (>40 m^2 sec^{-2}) near 15°S, 90°E. During the southern summer, disturbances form in the near equatorial southern hemisphere trough (Fig. 3) and propagate west-southwestward. Many of these disturbances become tropical storms as they move towards the Indian Ocean [Based on a global general circulation model, Manabe *et al.* (1970) investigated the generation mechanisms and structural features of tropical storms that developed over the Indian Ocean]. Bryant (1958) claimed that the activity of disturbances in the southern hemisphere monsoon trough is related in some way to changes in intensity of the northeasterly trades, flowing from the western North Pacific, through the Philippines, to the equatorial south China Sea and Malaysia.

4. Temporal variations of winter circulations

In this section, we will investigate the nature of the circulation changes that occurred during the northern winter of 1970-71. Fig. 6 is for the changes in $\bar{u}$ (top) and $\bar{v}$ (bottom) at 200 mb during the entire 90-day period. Since time series of daily $\bar{u}$ or $\bar{v}$ were found to contain day-to-day variations, a 3-day, weighted (0·25, 0·5, 0·25) running mean was applied to filter out short period fluctuations (Likewise, Figs. 7-9 are also for time series of 3-day running mean quantities).

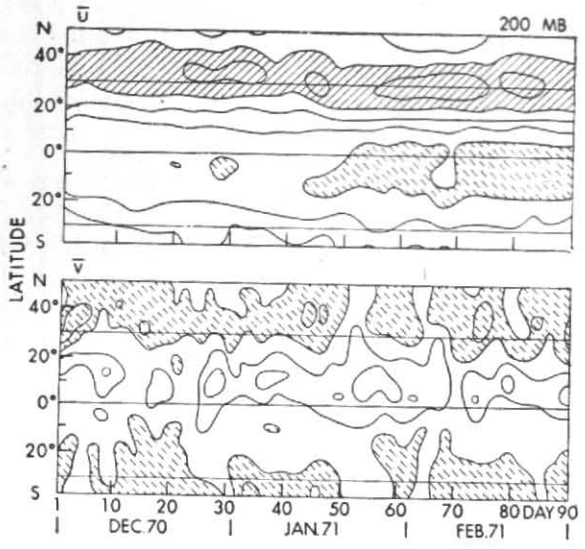

Fig. 6 (Top): Time-latitude section of 3-day running mean zonal wind $\bar{u}$ at 200 mb from December 1970 through February 1971. Interval 10 m sec^{-1}. Regions of $\bar{u} > 30$ m sec^{-1} are hatched, $\bar{u} < 0$ m sec^{-1} are dashed hatched.

(Bottom): Isopleths of 3-day running mean $\bar{v}$ at 200 mb. Interval 1 m sec^{-1}. Regions of negative (northerly) $\bar{v}$ are dashed hatched.

Fig. 6 (top) reveals that the jet stream, which had been centred near 35°N prior to day 45, shifted southwards to about 30°N at around that date. Almost concurrently, zonal mean easterlies developed in equatorial latitudes between 5°N and 15°S, accompanied by a somewhat rapid weakening of $\bar{u}$-westerlies near 30°S. When averaged over the entire 90-day period, $\bar{u}$ is weak and easterly ($\sim$1 m sec^{-1}) in a tropical region between 5°N and 15°S.

In general, $\bar{v}$ is positive (southerly) between about 20°S and 30°N with a maximum somewhere near 10°N. Poleward of 30°N $\bar{v}$ is usually negative (northerly). Thus the Hadley circulation is implied with its updraft portion to the south of 10°N downdraft centred around 30°N. As noted earlier in Fig. 2, the largest local contribution to this mean meridional Hadley cell is that due to N-S oriented overturnings over south-eastern Asia. Besides the thermally direct Hadley cell, we see the existence of indirect mean meridional cells associated with northerly $\bar{v}$ poleward of about 30°N and 20°S. Between about day 51 and 55, $\bar{v}$ is southerly at all latitudes from 35°S to 50°N; namely, the indirect cells seem to disappear from our region under study during that period. Thus an extensive mean Hadley cell encompassing latitudes very far to the north and south is implied. At 30°N, $\bar{v}$ is as large as 1·2 m sec^{-1} and southerly at day 53 as compared to its near zero season mean value.

It is probable that anomalous changes in $\bar{u}$ and $\bar{v}$ at 200 mb are associated with significant variations in the local upper winds. Beginning with Fig. 7, we investigate the changes in u at 200 mb along 37·1°N (top) and the equator (bottom). At 37·1°N, the jet stream to the east of Japan near 160°E became less than 20 m sec^{-1} around day 50 in contrast to its season mean value of 61 m sec^{-1}. After day 55, the jet stream recovered in intensity and reached a maximum ($>$100 m sec^{-1}) at about day 65. A glance at Fig. 7 (bottom) immediately reveals that conspicuous changes in the equatorial zonal winds occurred around day 55. Prior to that date, the equatorial easterlies over the eastern hemisphere (0° to 180°) never exceeded 20 m sec^{-1}. This is contrasted with frequent intensification of easterly winds to speeds above 20 m sec^{-1} after day 55. Similarly, the equatorial westerlies over the eastern Pacific near 130°W exceeded 30 m sec^{-1} more frequently prior to day 55 than after that day. These changes are well reflected in the $\bar{u}$ changes at the equator; namely, $\bar{u}$ became easterly after about day 50 (Fig. 6).

The most important finding in Fig. 7 is that sudden weakening of the jet stream near 160°E at 37·1°N occurred about 5 days prior to the wind shift at the equator. Does this indicate the importance of lateral coupling between higher and lower latitudes? In the present study, no attempt was made to answer this question. However, our speculation is that during the northern winter at 200 mb, such lateral coupling is most likely to occur over the central North Pacific near 130°W with a mid-oceanic upper trough embedded in the westerlies.

In this context, it may be of interest to see Fig. 8 (top) showing a time latitude section of u at 200 mb along 165°E. It exhibits an anomalous weakening of the jet stream around day 55. In fact, on that day, u is less than 40 m sec^{-1} near 30°-35°N where the season mean exceeds 60 m sec^{-1}. In spite of such an anomalous weakening of the mid-latitude westerlies, no significant u changes are noted in sub-tropical and tropical latitudes between about 25°N and the equator. As shown in Fig. 1, along 165°E the winds at 200 mb are westerly (easterly) to the north (south) of the sub-tropical ridge locating near 15°N. Most probably, the easterlies prohibit the equatorward penetration of mid-latitude effects.

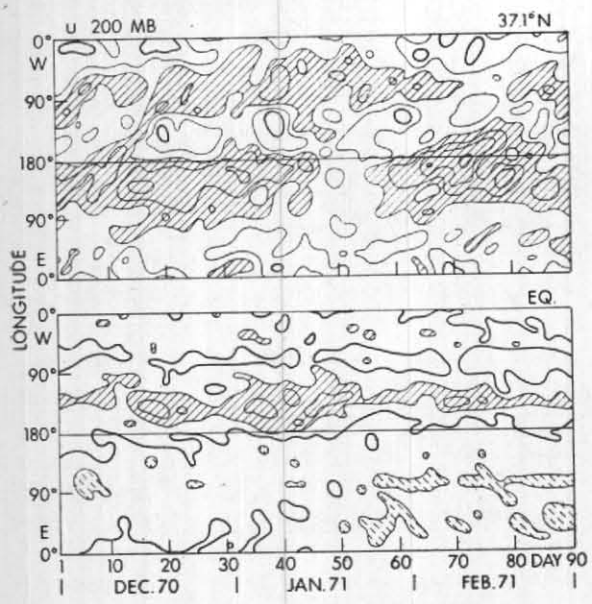

Fig. 7 (Top) : Time-longitude section of 3-day running mean u-component of wind at 200 mb along 37·1°N. Interval 20 m sec^{-1}. Regions of $u > 40$ m sec^{-1} are hatched.

(Bottom) : Isopleths of 3-day running mean u at 200 mb along the equator. Interval 15 m sec^{-1}. Regions of $u > 15$ m sec^{-1} are hatched, $u < -15$ m sec^{-1} are dashed hatched.

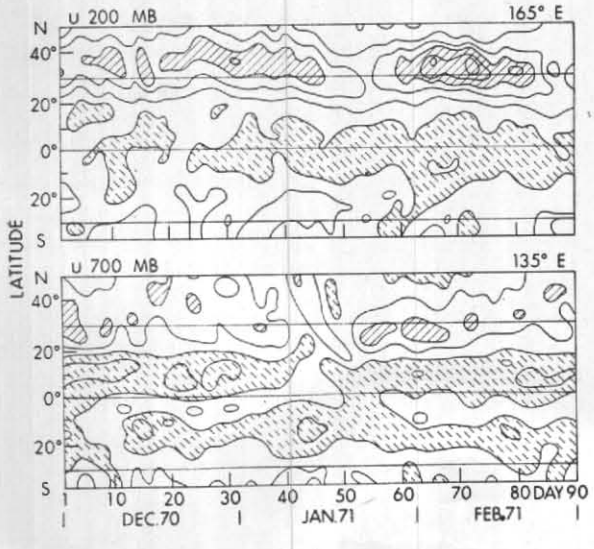

Fig. 8 (Top) : Time-latitude section of 3-day running mean 200 mb u at 165°E. Interval 20 m sec^{-1}. Regions of $u > 60$ m sec^{-1} are hatched, $u < 0$ are dashed hatched.

(Bottom) : Time-latitude section of 3-day running mean 700 mb u at 135°E. Interval 10 m sec^{-1}. Regions of $u > 20$ m sec^{-1} are hatched, $u < 0$ are dashed hatched.

This view may be supported by our previous finding that k^* at 200 mb is quite small equatorward of about 20°N along 165°E (Fig. 5, top).

Relatively large k^* at 700 mb along about 135°E (Fig. 5, bottom), perhaps, indicates the existence of active lateral coupling between mid-latitude and equatorial circulation regimes over the western North Pacific during the northern winter. In Fig. 8 (bottom), it is immediately apparent that the 700 mb winds near 10°N which should normally be easterlies are replaced by somewhat strong westerlies (~10 m sec^{-1}) between about day 43 and 47. It seems that during this period, near-equatorial westerlies are displaced from their normal position (~5°S) to the north of the equator. Concurrently, substantial intensification is noted in the southern hemisphere subtropical easterlies near 15°S as well as westerlies to the south of 30°S. This is in contrast to a considerable weakening of the northern hemisphere westerlies locating near 30°N. In fact, between about day 40 and 53 the westerlies at 30°N are less than 10 m sec^{-1} as compared with their season mean value of about 13 m sec^{-1}. In short, during the period between 43 and 47 day anomalous changes are observed over an extensive latitudinal zone covering both the northern and southern hemispheres. Whether such simultaneous fluctuations are really a result of significant interactions between the two hemispheres is a matter of conjecture and certainly worth further study. Yet another feature of interest in Fig. 8 (bottom) is that the near-equatorial westerlies, usually prevalent near 5°S, are completely wiped out from that region during the period between about day 50 and 56. Interestingly, this period is nearly coincident with that of an extremely weak jet stream at 200 mb around 30°N at 165°E (Fig. 8, top).

Fig. 9 is prepared to show anomalous features of cloudiness changes that occurred concurrently with abnormal u variations referred to earlier. Fig. 9 (top) exhibits a time-longitude section of cloudiness averaged over a tropical belt betweeen 5°N and 10°S. Cloudiness fluctuations are substantial over three major convective regions near 70°W, 115°E and 30°E. Of particular interest is the occurrence of large cloudiness (>6 okta) near 100°E-130°E during the period between about day 43 and 47. This is followed by a sharp cloudiness decrease from day 50 to 56. In fact, during this period cloudiness is well below normal over the Indonesian region. Similar features are noted in

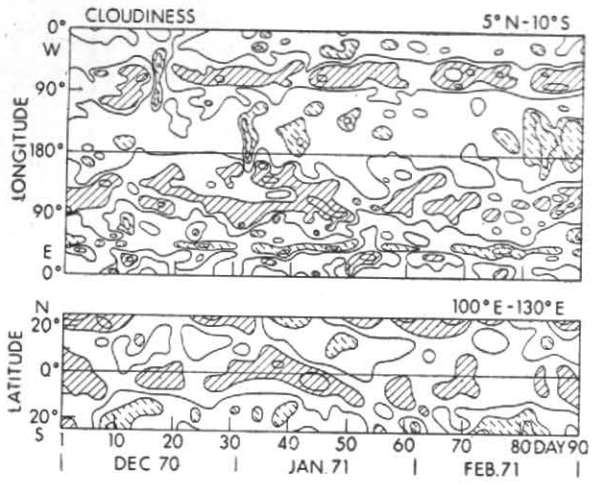

Fig. 9 (Top) : Time-longitude section of 3-day running mean cloudiness c averaged over a tropical belt between 5°N and 10°S. Interval 1 okta. Regions of $c>5$ okta are hatched, $c<3$ okta are dashed hatched.

(Bottom) : Time-latitude section of 3-day running mean c averaged over a region between 100°E and 130°E. Interval 1 okta. Regions of $c>5$ okta are hatched, $c<3$ okta are dashed hatched.

Fig. 9 (bottom) showing a time-latitude section of cloudiness averaged over a region between 100°E and 130°E; namely, near 5°S over that longitudinal region, extremely large cloudiness is found between about day 43 and 47 in contrast to very small cloudiness for day 50-57. In Fig. 9 (bottom) we also see the equatorward progression of a low cloudiness zone. This zone which was located at 25°N around day 40 reached as far south as the equator on about day 53. Perhaps, this low cloudiness zone may reflect depressed activity of surface cold air outbreaks in eastern Asia during that period. It is well known, among synoptic meteorologists, that monsoonal cold surges are associated with disturbance lines and enhanced rainfall (cloudiness) as they propagate equatorward.

We have so far shown that anomalous cloudiness changes over the Malaysian and Indonesian region are associated with considerable circulation anomalies over an extensive region covering both the northern and southern hemispheres. To facilitate further investigation, we have selected two contrasting five day periods; *i.e.*, day 43 to 47 (extremely wet over Malaysia and Indonesia), and day 50 to 54 (dry over the same region). Fig. 10 (a) depicts the distribution of cloudiness and Fig. 10 (b) 200 mb divergent winds during the former period. This is to be compared with Fig. 11 for the latter period.

Fig. 10 a (bottom) reveals that cloudiness is much about normal over an extensive region covering Malaysia, Indonesia, the equatorial Indian Ocean, and off the east and west coasts of Australia. In contrast, a well defined band of below normal cloudiness extends from south China, through Indochina and the western North Pacific, to the central South Pacific near 25°S, 150°W, crossing the equator to the east of New Guinea. In association with such anomalous cloudiness changes, the divergent winds at 200 mb appear to undergo rather drastic changes. A comparison between Figs. 2 and 10 b reveals the existence of abnormally strong convergence over the equatorial central Pacific near the dateline during the period from 12 to 16 January (or day 43-47), compatible with below normal cloudiness over that region. Associated with this is above normal upper outflow from the Indonesian region, congruent with cloudiness (rainfall) increase over that region. It appears that much of the upper outflows blows off toward the east as westerlies. In fact, the divergent westerlies along the equator are strongest ($\sim$3 m sec^{-1} at 160°E) during the period between 12 to 16 January. This, in turn, indicates that the Walker circulation is strongest during that period. Thus, it is probable that the intensified Walker circulation is largely responsible for carrying excess energy supplied over the Indonesian region a great distance downstream to the equatorial central Pacific dry zone, where cloudiness is below season's mean. On the other hand, the local Hadley cell between the divergent centre near Indonesia and convergent centre over north China appears to remain near or less than normal in intensity. This is well reflected in below normal cloudiness over eastern Asia (Fig. 10 a). Besides, the jet stream near Japan is much weaker than normal both at 200 mb and 700 mb as shown in Fig. 8. It is then tempting to speculate that the energy excess furnished around the Indonesian region due to abnormally large cloudiness (rainfall) is not transported northwards by means of the local Hadley cell to intensify the jet stream near Japan. Note in Figs. 8 and 9 that the occurrence of strong jet stream westerlies at around day 60 is simultaneous with near or below normal cloudiness over Malaysia and Indonesia.

We have previously shown that anomalous circulation changes were noted for the second 5-day period (50-54 day), too. We may summarize these features as follows : the extension of mean Hadley cell very far to the north and south (Fig. 6,

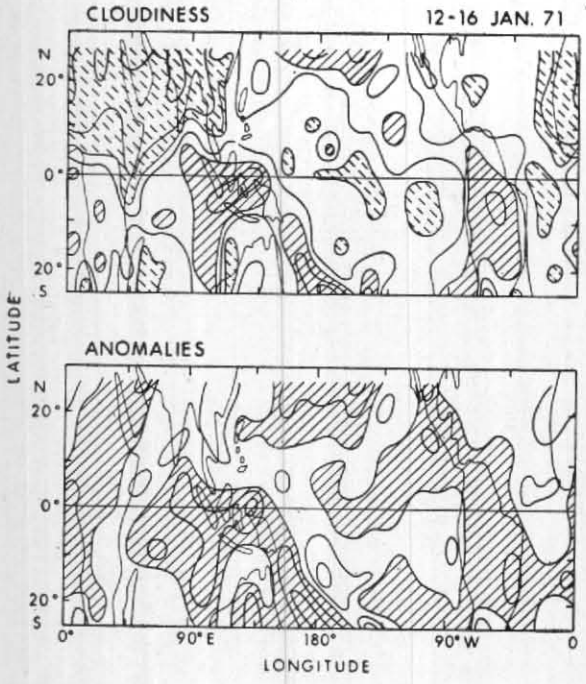

Fig. 10 (a) (Top) : Latitude-longitude section of cloudiness c averaged over the period 12-16 January 1971. Interval 1 okta. Regions of $c > 5$ okta are hatched, $c < 3$ okta are dashed hatched.

(Bottom) : Cloudiness anomaly computed by the difference between cloudiness for the period 12-16 January 1971 and that for the winter season mean. Interval 1 okta. Areas of positive anomaly are shaded.

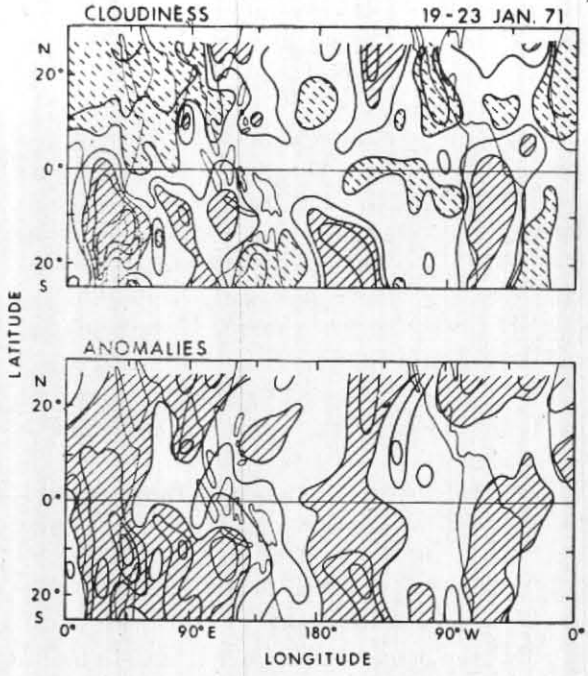

Fig. 11 (a). As in Fig. 10(a) but for period 19-23 January 1971.

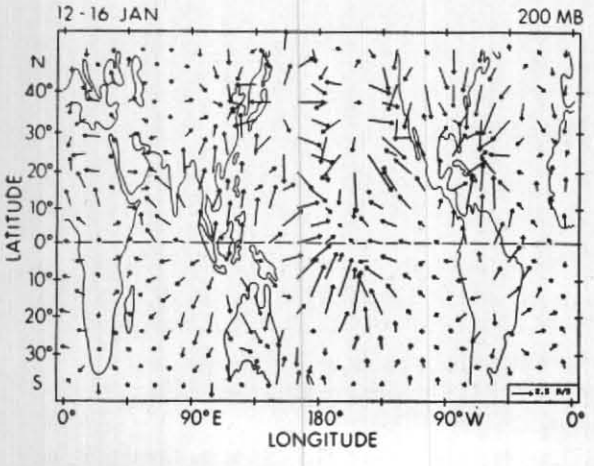

Fig. 10 (b). 200 mb divergent wind vector field for the period 12-16 January 1971.

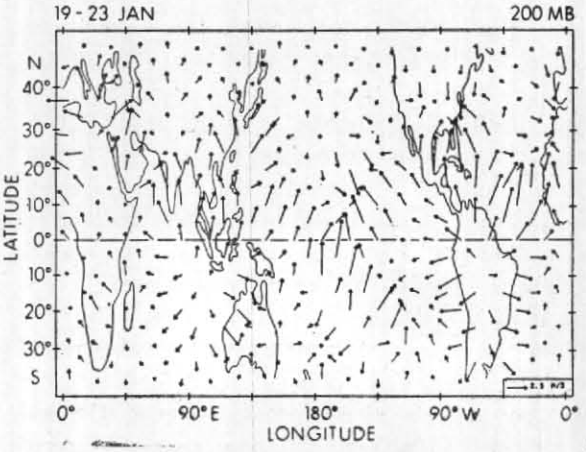

Fig. 11 (b). 200 mb divergent wind vector field for the period 19-23 January 1971.

bottom), unusual weakening of the jet stream at 200 mb near and east of Japan (Figs. 7 and 8), and the disappearance of near-equatorial westerlies at 700 mb near 5°S at 135°E (Fig. 8, bottom). We then turn our attention to Fig. 11(a), showing the distribution of cloudiness for 19-23 January 1971. Accompanying the disappearance of 700 mb near-equatorial westerlies, cloudiness is well below normal over Malaysia and Indonesia. In contrast well above normal cloudiness is found over the south Indian Ocean and South Africa between about 5°S and 15°S. Associated with this, the divergent centre at 200 mb (Fig. 11b), normally positioned near 2·5°S, 120°E, is displaced to about 10°S, 90°E over the south Indian Ocean. Over the equatorial Indian Ocean, substantial increase is encountered in the westerly winds at 700 mb (not shown). This is due to the equatorward penetration of a 700 mb trough, usually confined near India and to the north of a subtropical ridge axis along about 15°N (*see* Fig. 3). Of interest in Fig. 11(a) is the occurrence of large cloudiness (5·5 okta) near the southern tip of India where strong southerly winds prevail to the east of an intensified trough at 700 mb. In this region rainfall amount is not substantial during the northern winter. Occasionally, however, heavy rainfall appears to occur in association with the circulation changes in the upper westerlies both at 700 mb and 200 mb. In Fig. 7 (top), note that the westerly winds at 200 mb considerably decrease near 90°E at around day 50.

In Fig. 11(b), perceptible cross-equatorial southerly divergent winds exist over the central Pacific. Perhaps, this is largely associated with upper outflows originating from the South Pacific near 15°-20°S and between 140°W and 170°W, where cloudiness is more than 1 okta above season mean. Since the divergent winds over the central Pacific are predominantly meridional, the Walker circulation appears to be extremely weak, congruent with well below normal cloudiness over the Indonesian region. Similar features are also noted over the equatorial Indian Ocean, where the divergent part of the winds is more meridional than normal. Undoubtedly, the southerly divergent winds over that region are due to upper outflows from the south Indian Ocean where cloudiness is above normal. The predominance of southerly divergent flows are well reflected to the intensification of southerly $\bar{v}$ at the equator during the period from day 50 to 54 (Fig. 6, bottom). Conspicuously, the intensification of the mean Hadley cell during that period does not cause the increase in the $\bar{u}$ jet stream near 30°N (Fig. 6, top). This is a puzzling and challenging problem that requires further investigation.

5. Concluding remarks

Evidence has been presented that considerable cloudiness fluctuations occur during the northern winter over the Malaysian and Indonesian region, a key area for the MONEX Winter Experiment in 1979. It appears that these fluctuations occur in unison with large-scale circulation changes over a much more extensive area, covering both the northern and southern hemispheres, than just the immediate vicinity of Malaysia and Indonesia. However, it is not yet known as to exactly what the lateral (inter-hemispheric) and vertical interaction mechanisms may be. A comprehension of how regional weather changes mesh and interact with the large-scale winter circulation system is crucial to the success of MONEX. It is therefore imperative that the Winter Monsoon Experiment covers both regional and much larger scales, and the observational system be adequate to sense and resolve the changes in large scale winter monsoon flows to which the variations of regional circulations are related.

Acknowledgments

The authors are indebted to Mr. T. Grey, the Meteorological Satellite Laboratory, NOAA, for providing them NMC wind data for this study. Special thanks are due to Prof. Sadler for providing them with satellite observed cloudiness data during the period from December 1970 to February 1971. They also thank Mrs. S. Arita for typing the manuscript. This research has been supported by the Global Atmospheric Research Program, Climate Dynamic Research Section, National Science Foundation, under Grant No. ATM76-02502.

REFERENCES

Atkinson, G. D. and Sadler, J. C.	1970	Mean cloudiness and gradient-level wind charts over the tropics: Vol. I, Data Tech. Rep. 215, U.S. Air Weather Service, p. 48,
Bryant, K.	1958	*Met. Mag.*, **87**, pp. 307-312.
Krishnamurti, T. N., Kanamitsu, M., Koss, W. J. and Lee, J. D.	1973	A. *atmos. Sci.*, **30**, pp. 780 786.
Liang, G. T.	1974	The Climate of West Malaysia and Singapore, Oxford Univ. Press (Edited by O. J. Bee and C.L. Siu), pp. 31-35.
Manabe, S., Holloway, J. L. and Stone, H. M.	1970	*J. atmos. Sci.*, **27**, pp. 580-613.
Ramage, C. S.	1968	*Mon. Weath. Rev.*, **96**, pp. 365-370.
Sadler, J. C.	1968	Average cloudiness in the tropics from satellite observations, International Indian Ocean Expedition Met. Monogr. No. 2, East-West Center Press, Univ. Hawaii, 22 pp..

DISCUSSION

(Paper presented by M. S. Unninayar)

ABDUL LATIF HUNEIDI : Where is the core of sub-tropical jet stream mentioned by you over the east coast of the U.S.A. ? Does it have any relation with the Rocky Mountains jet stream ?

AUTHOR : The jet core lies at about 35°N, 80°W over the east coast of North America. It must inevitably be related to the westerlies over the Rockies.

P.R. PISHAROTY : What were the relative magnitudes of several values of divergent and non-divergent components of wind computed in the tropical belt 10°S to 10°N ?

AUTHOR : Divergent part of wind is approximately 1/10 of its non-divergent part in the tropical belt.

BOON KHEAN, CHEANG : As you have shown that during the period 16-22 January when there was weakening of E-W circulation, a tropical storm developed over the West Pacific. Do you think that there is any relation between these two features?

AUTHOR : There could be.